

# Gravitino Dark Matter and Light Element Abundances

Vassilis Spanos <sup>a</sup>

Department of Physics, University of Patras, GR-26500 Patras, Greece

**Abstract.** We discuss the scenario where the gravitino is the lightest supersymmetric particle and the long-lived next-to-lightest sparticle (NSP) is the neutralino or the stau, the charged partner of the tau lepton. In this case staus form bound states with several nuclei, affecting the cosmological abundances of  ${}^6\text{Li}$  and  ${}^7\text{Li}$  by enhancing nuclear rates that would otherwise be strongly suppressed. We consider the effects of these enhanced rates on the final abundances produced in Big-Bang nucleosynthesis (BBN), including injections of both electromagnetic and hadronic energy during and after BBN. We show that if the stau lifetime is longer than  $10^3 - 10^4$  s, the abundances of  ${}^6\text{Li}$  and  ${}^7\text{Li}$  are far in excess of those allowed by observations. For shorter lifetimes of order 1000 s, it appears that stau bound state effect could reduce the  ${}^7\text{Li}$  abundance from standard BBN values while at the same time enhancing the  ${}^6\text{Li}$  abundance, creating a region where both lithium abundances match their plateau values.

**PACS.** 11.30.Pb Supersymmetry – 95.35.+d Dark matter

## 1 Introduction

The primordial Big-Bang nucleosynthesis (BBN) predictions for the light elements abundance provide some of the most stringent constraints on the decays of unstable massive particles during the early Universe [1–8]. This is because the astrophysical determinations of the abundances of deuterium (D) and  ${}^4\text{He}$  agree well with those predicted by homogeneous BBN calculations, and also the baryon-to-photon ratio  $\eta \equiv n_b/n_\gamma \propto \Omega_b h^2$  needed for the success of these calculations [9,10] agrees very well with that inferred [11] from observations of the power spectrum of fluctuations in the cosmic microwave background (CMB). However, it is still difficult to reconcile the BBN predictions for the lithium isotope abundances with observational indications on the primordial abundances. The discovery of the “Spite” plateau [12], which demonstrates a near-independence of the  ${}^7\text{Li}$  abundance from the metallicity in Population-II stars, suggests a primordial abundance in the range  ${}^7\text{Li}/\text{H} \sim (1-2) \times 10^{-10}$  [13], whereas standard BBN with the CMB value of  $\eta$  would predict  ${}^7\text{Li}/\text{H} \sim 4 \times 10^{-10}$  [9,10]. In the case of  ${}^6\text{Li}$ , the data [14] lie a factor  $\sim 1000$  above the BBN predictions [15].

The effects of hadronic injections due to late decays of the NSP during BBN have also been studied extensively [3,5,6,16–21]. It has recently been pointed out that, if it has electric charge, the NSP forms bound states with several nuclei [22]. Due to the large NSP mass ( $m_{\text{NSP}} \gg m_{\text{nucleon}}$ ), the Bohr radii of these bound states  $\sim \alpha^{-1} m_{\text{nucleon}}^{-1} \sim 1$  fm are of order the nuclear size. Consequently, nuclear reactions with nuclei

in bound states are catalyzed, due to partial screening of the Coulomb barrier [23,24], and due to the opening of virtual photon channels in radiative capture reactions.

Here, we present results from a new analysis [8] that includes the nuclear reactions induced by hadronic and electromagnetic showers generated by late gravitational decays of the NSP, together with the familiar network of nuclear reactions used to calculate the primordial abundances of the light elements Deuterium (D),  ${}^3\text{He}$ ,  ${}^4\text{He}$  and  ${}^7\text{Li}$ . In addition, we include the effects of the bound states when the decaying particle is charged. We find that for lifetimes  $\tau < 10^3 - 10^4$  s, the enhanced rates of  ${}^6\text{Li}$  and  ${}^7\text{Li}$  production, exclude gravitino dark matter (GDM) with a stau NSP. At smaller lifetimes, we see that it is the  ${}^7\text{Li}$  destruction rates which are enhanced, facilitating a solution to the Li problems.

## 2 NSP Decays and resulting showers during BBN

In order to estimate the lifetime of the NSP, as well as the various branching ratios and the resulting EM and HD spectra, one must calculate the partial widths of the dominant relevant decay channels of the NSP. The decay products that yield EM energy obviously include directly-produced photons, and also indirectly-produced photons, charged leptons (electrons and muons) which are produced via the secondary decays of gauge and Higgs bosons, as well as neutral pions ( $\pi^0$ ). Hadrons (nucleons and mesons such as the  $K_L^0$ ,  $K^\pm$  and  $\pi^\pm$ ) are usually produced through the secondary decays of gauge and Higgs bosons, as well (for

<sup>a</sup> Email: vs Spanos@physics.upatras.gr

the mesons) as via the decays of the heavy  $\tau$  lepton. It is important to note that mesons decay before interacting with the hadronic background [3, 21]. Hence they are irrelevant to the BBN processes and to our analysis, except via their decays into photons and charged leptons. Therefore, the HD injections on which we focus our attention are those that produce nucleons, namely the decays via gauge and Higgs bosons and quark-antiquark pairs.

For the neutralino NSP  $\chi$ , we include the two-body decay channels  $\chi \rightarrow \tilde{G} H_i$  and  $\chi \rightarrow \tilde{G} V$ , where  $H_i = h, H, A$  and  $V = \gamma, Z$ . In addition, we include here the dominant three-body decays  $\chi \rightarrow \tilde{G} \gamma^* \rightarrow \tilde{G} q\bar{q}$ ,  $\chi \rightarrow \tilde{G} \gamma^* \rightarrow \tilde{G} W^+ W^-$ ,  $\chi \rightarrow \tilde{G} W^+ W^-$  and the corresponding interference terms. For the  $\tilde{\tau}$  NSP case, the lighter stau is predominantly right-handed, its interactions with  $W$  bosons are very weak (suppressed by powers of  $m_\tau$ ) and can be ignored. The decay rate for the dominant two-body decay channel, namely  $\tilde{\tau} \rightarrow \tilde{G} \tau$ , has been given in [25]. However, this decay channel *does not yield any nucleons*. Therefore, one must calculate some three-body decays of the  $\tilde{\tau}$  to obtain any protons or neutrons. The most relevant channels are  $\tilde{\tau} \rightarrow \tilde{G} \tau^* \rightarrow \tilde{G} Z \tau$ ,  $\tilde{\tau} \rightarrow Z \tilde{\tau}^* \rightarrow \tilde{G} Z \tau$ ,  $\tilde{\tau} \rightarrow \tau \chi^* \rightarrow \tilde{G} Z \tau$  and  $\tilde{\tau} \rightarrow \tilde{G} Z \tau$  [21].

Having calculated the partial decay widths and branching ratios, we employ the PYTHIA event generator [26] to model both the EM and the HD spectra of the NSP decays. These spectra and the fraction of the energy of the decaying particle that is injected as EM energy are then used to calculate the light-element abundances, as it is described in [8].

### 3 Bound-State Effects

On the other hand, it has recently been pointed out [22] that the presence of a charged particle, such as the stau, during BBN can alter the light-element abundances in a significant way due to the formation negatively charged staus of bound states (BS) with charged nuclei. The binding energies of these states are  $\alpha^2 Z_i^2 m_i / 2$   $\approx 30 Z_i^2 A_i$  keV, and the Bohr radii  $\sim (\alpha Z_i m_i) \sim 1 Z_i^{-1} A_i^{-1}$  fm. For species such as  ${}^4\text{He}$ ,  ${}^7\text{Li}$  and  ${}^7\text{Be}$ , these energy and length scales are close to those of nuclear interactions, and it thus turns out that bound state formation results in catalysis of nuclear rates via two mechanisms.

One immediate consequence of the bound states is a reduction of the Coulomb barrier for nuclear reactions, due to partial screening by the stau. Since Coulomb repulsion dominates the charged-particle rates, all such rates are enhanced. An additional effect enhances radiative capture channels  $A_2(A_1, \gamma)X$  by introducing photonless final states in which the stau carries off the reaction energy transmitted via virtual photon processes. In particular, the  ${}^4\text{He}(d, \gamma){}^6\text{Li}$  reaction, which is suppressed in standard BBN, is enhanced by many orders of magnitude by the presence of the bound states. As described in [22], the virtual photon channel has a cross section which is enhanced

over that of the usual radiative capture cross section by  $\frac{\sigma_{\text{CBBN}}}{\sigma_{\text{SBBN}}} \sim (a\omega)^{-n}$ , where  $a$  is the BS Bohr radius and  $\omega = \lambda^{-1}$  is the photon energy. The index  $n$  depends on the type of transition multipole: for (E1, E2) transitions,  $n = (3, 5)$ . To account for bound state effects, an accurate calculation of their abundance is necessary. To do this we solve numerically the Boltzmann equations (13) and (14) from [23], that control these abundances.

### 4 Results and Discussion

Our framework is CMSSM and mSUGRA models [27], where the NSP could be either the lighter stau or the lightest neutralino. We start presenting results based on CMSSM models with  $A_0 = 0$ ,  $\mu > 0$  and  $\tan \beta = 10$ , showing explicit element abundance contours. In Fig. 1a, we show the element abundances that result when the gravitino mass is held fixed at  $m_{3/2} = 100$  GeV in the presence of stau bound state effects. To the left of the near-vertical solid black line at  $m_{1/2} \simeq 250$  GeV, the gravitino is the not the LSP, and we do not consider this region here. The diagonal red dotted line corresponds to the boundary between a neutralino and stau NSP. Above the line, the neutralino is the NSP, and below it, the NSP is the stau. Very close to this boundary, there is a diagonal brown solid line. Above this line, the relic density of gravitinos from NSP decay is too high, i.e.,  $(m_{3/2}/m_{\text{NSP}})\Omega_{\text{NSP}} h^2 > 0.12$ . Thus we should restrict our attention to the area below this line. Note that we display the extensions of contours which originate below the line into the overdense region, but we do not display contours that reside solely in the upper plane.

The very thick green line labelled  ${}^7\text{Li} = 4.3$  corresponds to the contour where  ${}^7\text{Li}/\text{H} = 4.3 \times 10^{-10}$ , a value very close to the standard BBN result for  ${}^7\text{Li}/\text{H}$ . There are additional (unlabeled) thin green contours showing  ${}^7\text{Li}/\text{H} = 2 \times 10^{-10}$  (dashed). For this case with  $m_{3/2} = 100$  GeV the  ${}^6\text{Li}$  abundance is never sufficiently high to match the observed  ${}^6\text{Li}$  plateau for the same parameter values where  ${}^7\text{Li}$  is reduced. The  ${}^6\text{Li}/{}^7\text{Li}$  ratio is shown by the solid blue contour labeled  ${}^6\text{Li}/{}^7\text{Li} = 0.15$ . At large  $m_{1/2}$ , the contour for  ${}^6\text{Li}/{}^7\text{Li} = 0.01$  is shown by the thin blue line. To the right of this contour, including the region where  ${}^7\text{Li} \sim 2 \times 10^{-10}$ , the  ${}^6\text{Li}$  abundance is too small. Finally, we show the contours for  $\text{D}/\text{H} = 2.2$  and  $4.0 \times 10^{-5}$  by the solid purple contours as labeled. The  $\text{D}/\text{H} = 2.2 \times 10^{-5}$  contour is a small loop within the  ${}^6\text{Li}/{}^7\text{Li}$  loop. Inside this loop  $\text{D}/\text{H}$  is too small. Between the two curves labeled 4.0, the  $\text{D}/\text{H}$  ratio is high, but not necessarily excessively so. As a better illustration of our results, we have shaded as orange (lighter) the region where the differences between the calculated and observed light-element abundances are no greater than in standard BBN without late particle decays, that is  ${}^3\text{He}/\text{D} < 1$ ,  ${}^6\text{Li}/{}^7\text{Li} < 0.15$ ,  $2.2 \times 10^{-5} < \text{D}/\text{H} < 4.0 \times 10^{-5}$  and  ${}^7\text{Li}/\text{H} < 4.3 \times 10^{-10}$ . Only when  $m_{1/2} \gtrsim 3500 - 4000$  GeV does the  $\text{D}/\text{H}$  abundance drop back to acceptable

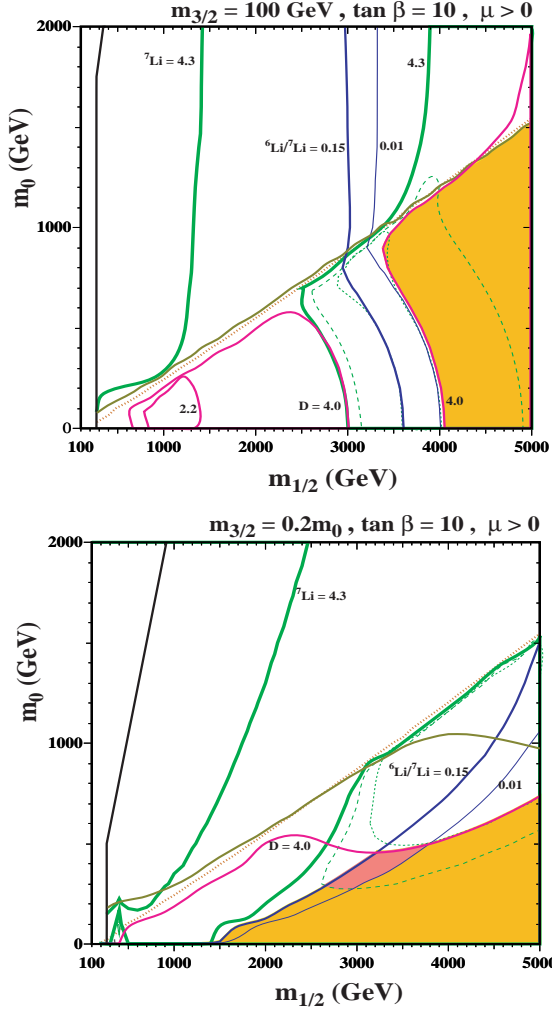


**Fig. 1.** The  $(m_{1/2}, m_0)$  planes for  $A_0 = 0$ ,  $\mu > 0$  and  $\tan \beta = 10$ . In the upper (lower) panel we use  $m_{3/2} = 100$  GeV ( $m_{3/2} = 0.2 m_0$ ). The regions to the left of the solid black lines are not considered, since there the gravitino is not the LSP. In the orange (light) shaded regions, the differences between the calculated and observed light-element abundances are no greater than in standard BBN without late particle decays. In the pink (dark) shaded region in the lower panel the the lithium abundances match the observational plateau values. The significance of the other contours is explained in the text. In these figures we have incorporated the bound-state effects.

levels with good abundances for  ${}^7\text{Li}$ , but  ${}^6\text{Li}$  is now too small to account for the plateau. Thus, for a constant value of  $m_{3/2} = 100$  GeV, the bound-state effects force one to extremely large values of  $m_{1/2}$  primarily due to the enhanced production of  ${}^6\text{Li}$ , as shown by the orange shaded region. For this value of the gravitino mass, there are no regions where both lithium abundances match their plateau values.

In Fig. 1b, we fix  $m_{3/2} = 0.2 m_0$  and neglect the bound-state effects. The choices of contours are similar to the upper panel. The gravitino relic density constraint now cuts out some of the stau NSP re-

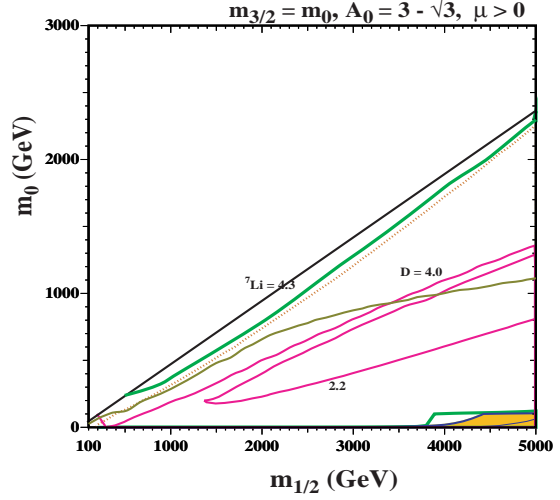


**Fig. 2.** The  $(m_{1/2}, m_0)$  plane for  $mSUGRA$  with  $m_{3/2} = m_0$  and  $A_0/m_0 = 3 - \sqrt{3}$  as in the simplest Polonyi superpotential. The various contours and regions are as in Fig. 1.

gion at large  $m_{1/2}$  and large  $m_0$ , but allows a small neutralino NSP region at low  $m_{1/2}$ . In this case the constraint from  ${}^3\text{He}/\text{D}$  is not very strong in the stau NSP region and the contour is not shown. The region where the  ${}^6\text{Li}/{}^7\text{Li}$  ratio lies between 0.01 and 0.15 now forms a band which moves from lower left to upper right. Thus, as one can see in the orange shading, there is a large region where the lithium isotopic ratio can be made acceptable. However, if we restrict to  $D/\text{H} < 4.0 \times 10^{-5}$ , we see that this ratio is interesting only when  ${}^7\text{Li}$  is at or slightly below the standard BBN result. Once again, we see that the increased production of both  ${}^6\text{Li}$  and  ${}^7\text{Li}$  excludes a portion of the stau NSP region where  $m_{1/2} \lesssim 1500$  GeV for small  $m_0$ . The lower bound on  $m_{1/2}$  increases with  $m_0$ . In this case, not only do the bound-state effects increase the  ${}^7\text{Li}$  abundance when  $m_{1/2}$  is small (i.e., at relatively long stau lifetimes), but they also decrease the  ${}^7\text{Li}$  abundance when the lifetime of the stau is about 1500 s. Thus, at  $(m_{1/2}, m_0) \simeq (3200, 400)$ , we find that  ${}^6\text{Li}/{}^7\text{Li} \simeq 0.04$ ,  ${}^7\text{Li}/\text{H} \simeq 1.2 \times 10^{-10}$ , and  $D/\text{H} \simeq 3.8 \times 10^{-5}$ . Indeed, when  $m_{1/2}$  is between 3000-4000 GeV, the bound state effects cut the  ${}^7\text{Li}$  abundance roughly in half. In the darker (pink) region the lithium abundances match the observational plateau values, with the properties  ${}^6\text{Li}/{}^7\text{Li} > 0.01$  and  $0.9 \times 10^{-10} < {}^7\text{Li}/\text{H} < 2.0 \times 10^{-10}$ .

Finally, we come to an example of a  $mSUGRA$  model in Fig. 2. Here, because of a relation between the bilinear and trilinear supersymmetry breaking terms:  $B_0 = A_0 - m_0$ ,  $\tan \beta$  is no longer a free parameter of the theory, but instead must be calculated at each point of the parameter space. Here, we choose an example based on the Polonyi model for which  $A_0/m_0 = 3 - \sqrt{3}$ . In addition, we have  $m_{3/2} = m_0$ . The upper part of the plane, we do not have GDM. We note that  ${}^6\text{Li}$  is interestingly high, between 0.01

and 0.15 in much of this region. Due to the bound-state effects both lithium isotope abundances are too large except in the extreme lower right corner, where there is a small region shaded orange. Henceforth, the BBN constraints and the bound state effects practically exclude the bulk of the parameter space of this simple Polonyi SUGRA model.

## 5 Conclusions

We discussed the cosmological light-element abundances in the presence of the electromagnetic and hadronic showers due to late decays of the NSP in the context of the CMSSM and mSUGRA models, incorporating the effects of the bound states that would form between a metastable stau NSP and the light nuclei. Late decays of the neutralino NSP constrain significantly the neutralino region, since in general they yield large light-element abundances. The bound-state effects are significant in the stau NSP region, where excessive  ${}^6\text{Li}$  and  ${}^7\text{Li}$  abundances exclude regions where the stau lifetime is longer than  $10^3 - 10^4$  s. For lifetimes shorter than 1000 s, there is a possibility that the stau decays can reduce the  ${}^7\text{Li}$  abundance from the standard BBN value, while at the same time enhancing the  ${}^6\text{Li}$  abundance, defining a region where both lithium abundances match their plateau values.

## Acknowledgments

This work was supported by Marie Curie International Reintegration grant “SUSYDM-PHEN”, MIRC-CT-2007-203189 and the Marie Curie Excellence grant MEXT-CT-2004-014297. We also acknowledge support from the Research Training Network “HEPTOOLS”, MRTN-CT-2006-035505.

## References

1. E. Holtmann, M. Kawasaki, K. Kohri and T. Moroi, Phys. Rev. D **60**, 023506 (1999) [arXiv:hep-ph/9805405].
2. M. Kawasaki, K. Kohri and T. Moroi, Phys. Rev. D **63** (2001) 103502 [arXiv:hep-ph/0012279].
3. K. Kohri, Phys. Rev. D **64** (2001) 043515 [arXiv:astro-ph/0103411].
4. R. H. Cyburt, J. R. Ellis, B. D. Fields and K. A. Olive, Phys. Rev. D **67** (2003) 103521 [arXiv:astro-ph/0211258].
5. M. Kawasaki, K. Kohri and T. Moroi, Phys. Lett. B **625** (2005) 7 [arXiv:astro-ph/0402490]; Phys. Rev. D **71** (2005) 083502 [arXiv:astro-ph/0408426].
6. K. Kohri, T. Moroi and A. Yotsuyanagi, Phys. Rev. D **73**, 123511 (2006) [arXiv:hep-ph/0507245].
7. K. Jedamzik, Phys. Rev. D **74** (2006) 103509 [arXiv:hep-ph/0604251].
8. R. H. Cyburt, J. R. Ellis, B. D. Fields, K. A. Olive and V. C. Spanos, JCAP **0611** (2006) 014 [arXiv:astro-ph/0608562].
9. R. H. Cyburt, B. D. Fields and K. A. Olive, New Astron. **6** (2001) 215 [arXiv:astro-ph/0102179].
10. R. H. Cyburt, B. D. Fields and K. A. Olive, Phys. Lett. B **567**, 227 (2003); A. Coc, E. Vangioni-Flam, P. Descouvemont, A. Adahchour and C. Angulo, Astrophys. J. **600** (2004) 544 [arXiv:astro-ph/0309480]; B.D. Fields and S. Sarkar in: S. Eidelman *et al.* [Particle Data Group], Phys. Lett. B **592**, 1 (2004); R. H. Cyburt, Phys. Rev. D **70** (2004) 023505 [arXiv:astro-ph/0401091].
11. R. H. Cyburt, B. D. Fields and K. A. Olive, Astropart. Phys. **17** (2002) 87 [arXiv:astro-ph/0105397].
12. F. Spite, M. Spite, Astronomy & Astrophysics, **115** (1992) 357.
13. S. G. Ryan, T. C. Beers, K. A. Olive, B. D. Fields, and J. E. Norris Astrophys. J. Lett. **530** (2000) L57 [arXiv:astro-ph/9905211].
14. R. Cayrel, M. Spite, F. Spite, E. Vangioni-Flam, M. Cassé, and J. Audouze, Astron. Astrophys. **343**, 923 (1999); M. Asplund, D. L. Lambert, P. E. Nissen, F. Primas and V. V. Smith, Astrophys. J. **644**, 229 (2006) [arXiv:astro-ph/0510636].
15. D. Thomas, D. N. Schramm, K. A. Olive and B. D. Fields, Astrophys. J. **406**, 569 (1993) [arXiv:astro-ph/9206002].
16. K. Jedamzik, Phys. Rev. Lett. **84**, 3248 (2000).
17. K. Jedamzik, Phys. Rev. D **70** (2004) 063524 [arXiv:astro-ph/0402344]; K. Jedamzik, Phys. Rev. D **70** (2004) 083510 [arXiv:astro-ph/0405583].
18. F. D. Steffen, JCAP **0609** (2006) 001 [arXiv:hep-ph/0605306]; J. Pradler and F. D. Steffen, arXiv:0710.4548 [hep-ph].
19. M. Kawasaki, K. Kohri and T. Moroi, Phys. Lett. B **649** (2007) 436 [arXiv:hep-ph/0703122].
20. J. R. Ellis, K. A. Olive and E. Vangioni, Phys. Lett. B **619**, 30 (2005) [arXiv:astro-ph/0503023].
21. J. L. Feng, A. Rajaraman and F. Takayama, Phys. Rev. D **68** (2003) 063504 [arXiv:hep-ph/0306024]; J. L. Feng, S. f. Su and F. Takayama, Phys. Rev. D **70** (2004) 063514 [arXiv:hep-ph/0404198]; J. L. Feng, S. Su and F. Takayama, Phys. Rev. D **70** (2004) 075019 [arXiv:hep-ph/0404231].
22. M. Pospelov, Phys. Rev. Lett. **98** (2007) 231301 [arXiv:hep-ph/0605215]; C. Bird, K. Koopmans and M. Pospelov, arXiv:hep-ph/0703096.
23. K. Kohri and F. Takayama, Phys. Rev. D **76** (2007) 063507 [arXiv:hep-ph/0605243].
24. M. Kaplinghat and A. Rajaraman, Phys. Rev. D **74** (2006) 103004 [arXiv:astro-ph/0606209].
25. J. R. Ellis, K. A. Olive, Y. Santoso and V. C. Spanos, Phys. Lett. B **588** (2004) 7 [arXiv:hep-ph/0312262].
26. T. Sjostrand, P. Eden, C. Friberg, L. Lonnblad, G. Miu, S. Mrenna and E. Norrbin, Comput. Phys. Commun. **135** (2001) 238 [arXiv:hep-ph/0010017].
27. J. R. Ellis, K. A. Olive, Y. Santoso and V. C. Spanos, Phys. Lett. B **573** (2003) 162 [arXiv:hep-ph/0305212]; J. R. Ellis, K. A. Olive, Y. Santoso and V. C. Spanos, Phys. Rev. D **70** (2004) 055005 [arXiv:hep-ph/0405110].